Heliyon 6 (2020) e04128

Contents lists available at ScienceDirect

Heliyon

journal homepage: www.cell.com/heliyon

Research article

Nb_2O_5 supported in mixed oxides catalyzed mineralization process of methylene blue

Gustavo Senra Gonçalves de Carvalho, Marcelo Magno de Siqueira, Maria Patrícia do Nascimento, Marcone Augusto Leal de Oliveira, Giovanni Wilson Amarante *

Federal University of Juiz de Fora, Chemistry Department, Cidade Universitária, Rua José Lourenço Kelmer s/n, Juiz de Fora, MG, 36036-900, Brazil

ARTICLE INFO

Keywords:
Supported niobium oxide
Photocatalysis
Sunlight
Organic dye
Degradation
Spectroscopy
Heterogeneous catalysis
Photochemistry
Water pollution
Water quality
Environmental science
Chemistry

ABSTRACT

Heterogeneous photocatalysis has become a significant green technology for water treatment. The application of Nb_2O_5 catalyst for the photodegradation of contaminants has merged as an important tool to this process. Furthermore, it is known that catalytic phases supported on metal oxides are an alternative method for enhancing its activity. In this work, supported Nb_2O_5 on mixed oxides as catalyst was applied to degrade methylene blue dye, leading to almost 100% of dye degradation without the need of any additives, after only three hours of sunlight exposure. The effect of catalyst concentration, exposure time and light source were investigated. The best catalyst activity was found at 1.5 g L^{-1} and for higher catalyst concentrations the degradation was kept constant. Plausible intermediates of this degradation process were observed and characterized by NMR, LC/MS and CZE techniques. After degradation, the catalyst was recovered and could be further re-applied in other three reaction cycles without significant loss of catalytic activity.

1. Introduction

Large amounts of dyes are produced and used annually in different industries including textiles, cosmetics, paper, leather, pharmaceuticals, and nutrition. There are more than 100,000 commercially available dyes with an annual production estimate of more than 70,000 tons, of which 15% are lost during the dyeing process [1, 2, 3, 4, 5]. In addition, traces of dyes in effluents are highly visible and undesirable, leading to damage to aquatic life and disturbances in human health. These concerns have led to stringent regulations on wastewater disposal as well as the development of more efficient treatment technologies. Besides, the optimization of water use in productive processes has been receiving special attention due to its high cost and restrictions imposed for legislation in terms of both abstraction and disposal [6]. The release of colored wastewater into the ecosystem without appropriate treatment causes aesthetic pollution, eutrophication, and disturbances in aquatic life. As international environmental standards are becoming more stringent, these untreated, colored waste disposal practices are no longer accepted anymore [7].

Several methods have been suggested to solve this problem of water dye removal, such as biodegradability, coagulation, adsorption, and osmotic processes [1, 2, 3, 4, 5, 8, 9]. All these processes have some advantages or disadvantages over the others. However, these conventional methods are non-destructive, since they only transfer the organic contaminant into another problem giving rise to a new type of pollution, which also requires a treatment [8].

In this context, advanced oxidation processes (AOP) have emerged as potential destructive method against highly resistant molecules. Among the AOP, the heterogeneous photocatalysis using semiconductor materials appears prominently. The main advantage of the photocatalytic process is its inherent destructive nature; can occur at ambient conditions (atmospheric oxygen is adequate as oxidant) and can lead to complete mineralization of organic molecules into CO_2 [1-5,8,9]. In such methodologies, pure or doped metal oxide semiconductors (e.g. TiO_2, ZnO and Nb_2O_5) are commonly used as photocatalysts [8, 10, 11]. Several studies reported the use of TiO_2 and ZnO for treating wastewater due to their characteristics, such as relative high efficiency, low cost, and nontoxicity [1, 2, 3, 4, 5]. However, due to its similar properties, the application of Nb_2O_5 as photocatalyst of dye degradation has been reported and appeared as an interesting alternative. As an important advantage, generally Nb_2O_5 requires less separation steps and higher recycling rate,

* Corresponding author.
E-mail address: giovanni.amarante@ufjf.edu.br (G.W. Amarante).

https://doi.org/10.1016/j.heliyon.2020.e04128
Received 3 April 2020; Received in revised form 7 May 2020; Accepted 1 June 2020

an important parameter for industrial process [8, 10, 12]. In addition, several methodologies have been explored these semiconductors aiming new processes, among them, morphological modification [8, 13] and doped materials [11] can be highlighted.

In this scenario, Nb_2O_5 can be used on the surface of some metallic oxides in order to shift the absorption of radiation towards higher wavelengths [9, 14, 15, 16]. It is worth mentioning that the characteristics of the support must be considered to increase the surface area and the rate of the reaction. However, considerable modifications in the properties of the supported oxides may occur due to the interaction with the support [17]. Among the materials that can be used as supports for the semiconductor catalysts are the mixed oxides derived from layered double hydroxides (LDH). LDHs have a natural occurrence but can also be synthesized by simple and low-cost routes, allowing their isolation as high-purity solids. Generally, the products formed by the thermal decomposition of the LDHs present a great increase in the superficial area, in the volume and pores, special micro-structure and high pH [18, 19, 20]. It is worth noting that the LDH with zinc oxide in its structure has been used in photodegradation of dyes [13]. Based on this principle, we envisioned the potential of this material for dye photodegradation.

Herein, a Nb_2O_5 supported in mixed oxides as catalyst for photocatalytic degradation of methylene blue (MB) is presented. Moreover, the degradation rate, recycle and photocatalytic degradation pathway are also discussed. Finally, after only 3 h exposure of sun light irradiation leads to complete degradation of this highly resistant organic dye.

2. Experimental

2.1. Catalyst synthesis and characterization

The catalyst synthesis was performed according to literature protocol [21]. This methodology consists of the following steps: First, the synthesis of the layered double hydroxide (LDH) was carried out via the co-precipitation method. 0.5 L of an aqueous solution of NaOH (10.16 g, 254 mmol, 6.35 equiv.) and Na_2CO_3 (2.69 g, 25.4 mmol, 0.65 equiv.) was slowly added to 0.5 L of an aqueous solution containing aluminum nitrate salt (15.0 g, 40 mmol of $Al(NO_3)_3.9H_2O$, 1 equiv.) and 40 mmol (11.90 g, 1 equiv.) of $Zn(NO_3)_2.6H_2O$ and then stirred at room temperature for 24 h. The precipitate was then filtrated and washed with distilled water until a neutral pH was reached, leading the LDH with the formula $[Zn_{0.67}Al_{0.33}(OH)_2(CO_3)_{0.165}].nH_2O$ [22, 23]. Then, the mixed oxide was obtained by calcination of the corresponding LDH at temperature of 500 °C for 5 h (soak time) with heating rate of 20 °C min^{-1} (ramp time) to give a white crystalline powder with proposed molecular formula $[Zn_{0.67}Al_{0.33}O]$ or $[5ZnO.ZnAl_2O_4]$. Finally, the catalyst was then prepared by impregnation methodology, taking the support with ammoniacal niobium oxalate aqueous solution. The niobium loading was theoretically calculated by taking 2 mmol of ammoniacal niobium oxalate which affords 1 mmol of Nb_2O_5 after heating. Thus, 270 mg of the mixed oxide, and 30 mg (0.113 mmol) of Nb_2O_5 was desired (and, consequently, 89 mg (0.226 mmol) of the niobium precursor was employed). Finally, the resulting material was calcined at 500 °C to obtain the desired catalyst with the proposed molecular formula $[(4ZnO)(1.5ZnAl_2O_4)]_{100}(Nb_2O_5)_{20}(H_2O)_5$ [21].

The LDH, mixed oxide and the catalyst were fully characterized through analyses of SSNMR of nuclei ^{27}Al and ^{13}C, diffractograms patterns, I.R., RAMAN spectroscopies and ICP-OES and all data are consistent in comparison to literature [21]. ^{27}Al SSNMR spectrum of the LDH shows characteristic aluminum signals from octahedral sites (AlO_6 – δ 14.20 ppm) with a slightly change on the typically shield, probably caused by the presence of zinc. ^{13}C SSNMR spectrum shows characteristic carbonate ions signals at 170 ppm, likely present in the interlayer medium. The diffractogram presents peaks characteristic of hydrotalcite-type materials, with reflection 2θ in approximately 11.60° referring to *003* plane. IR spectrum shows mainly signals related to interlayer carbonates, with band at approximately 1600 cm^{-1}, and band in the region of 500 cm^{-1} referring to the metal-oxygen bonds. Raman spectrum presents bands at 1065 and 1050 cm^{-1} relative to symmetrical stretching of carbonate ions.

The ^{27}Al SSNMR spectrum of the mixed oxide shows signal in the region near δ 9.0 ppm, which is characteristic of aluminum at octahedral sites (AlO_6). However, differently than the LDH precursor, it appears a peak at approximately δ 67.0 ppm, corresponding to aluminum at AlO_4 sites. In addition, a signal in the region of δ 49.0 ppm was observed, which is characteristic of aluminum in distorted tetrahedral sites. It is important to mention, the presence of Zn^{2+} causes this effect, due to the two crystalline phases after calcination. The powder X-ray diffraction pattern also suggests the formation of ZnO phase and the distinct AlO_4 environments as well. Peaks 2θ (CuKα) around 33° (100), 34° (002), 36.5° (101), 48° (102), 57° (110), 63° (103), 69° (112) are consistent with ZnO. IR spectrum of the mixed oxide shows band in the region of 500 cm^{-1}, corresponding to the symmetrical stretching of metal-oxygen bonds. Absence of signals such as carbonates, waters and hydroxyls groups, previously observed in the LDH precursor, is now highlighted.

The ^{27}Al SSNMR spectrum of the supported niobium oxide catalyst showed a similar profile to the mixed oxide precursor, with aluminum at octahedral sites (AlO_6 – δ 5.0–11.0 ppm), AlO_4 sites (δ 70.0 ppm) and aluminum in distorted tetrahedral sites (δ 49.0 ppm). The XRD analysis was performed aiming to identify different crystalline phases on the support. The patterns have wide lines related to the low crystallinity of mixed oxides. After the addition of niobium, no major differences were observed in comparison to the support, indicating good dispersion of these particles on the mixed oxides surface. The Raman spectrum of alumina supported niobium oxide presented broad bands around 860–950 cm^{-1}, that were absent in the support. Inductively Coupled Plasma-Atomic Emission Spectrometry (ICP-OES) analysis revealed the presence of 4.5% of niobium in the catalyst. The chemical analysis for the catalysts also revealed a good correlation with the expected structures, suggesting an aluminum content around 12 wt% and zinc 60% in weight.

2.2. Dye degradation tests

The methylene blue (MB) photodegradation experiments were carried out by modifying the methodology described in the literature [10, 13], which consists basically in the preparation of a solution of the dye of MB, in a concentration of 25 μmol L^{-1} and add to it the catalyst. The photocatalytic activity of the catalyst was monitored by the degradation of MB under irradiation with UVA light in a chamber designed by Vaz *et al* [24] at room temperature and by sunlight exposure. A UV-Vis Shimadzu UV-1800 spectrophotometer with a spectral range between 200-800 nm was used, using 1.0 nm quartz cuvettes to monitoring the degradation processes. The measurements in the spectrophotometer were done after intervals of radiation exposure, in triplicate. To measure the samples concentrations, a calibration curve was prepared by varying methylene blue concentration in 6 levels between 1 and 25 μM, all in triplicate. The calibration curve was constructed from the linear regression between the points obtained at 664 nm, wavelength of maximum absorbance.

2.3. NMR spectroscopy, mass spectrometry and capillary zone electrophoresis analyses

^1H NMR spectra were obtained at 11.7 T on a Bruker Avance III HD 500 spectrometer operating at a Larmor frequency of 500 MHz. The sample solution was prepared in appropriated deuterated solvent D_2O, at a MB concentration of 3 mg mL-1 - necessary to obtain a high-resolution spectrum – and was exposed to optimized degradation conditions. For NMR spectrum acquisition an aliquot of 5 μL was analyzed.

Mass spectrometry characterization of the compounds was performed in 6120 Quadrupole LC/MS (Agilent Technologies, Singapore) equipped with an API-ES ion source, coupled to an Agilent CE 7100 Capillary Electrophoresis instrument (Agilent Technologies, Singapore). The

Table 1. Percentage of degradation of MB in optimization experiments.*

Reaction conditions	% Degradation
Catalyst conc. 0.5 mg mL^{-1}	39.48
Catalyst conc. 1.0 mg mL^{-1}	43.60
Catalyst conc. 1.5 mg mL^{-1}	62.48
Catalyst conc. 2.0 mg mL^{-1}	51.92
Niobium oxide	30.28
Support	33.04
Cycle 1	62.48
Cycle 2	59.96
Cycle 3	53.60
5 min UV Box	25.32
5 min Sunlight	43.40
30 min UV Box	38.32
30 min Sunlight	60.28
60 min UV Box	62.48
60 min Sunlight	78.20

* Unless notified all reactions were carried out for 60 min and with catalyst concentration 1.5 mg mL^{-1}.

Table 2. Comparison of percentage of degradation of MB with UVA and sunlight.

Time (min.)	% Degradation	
	UV Box	Sunlight
5	25.32	43.40
30	38.32	60.28
60	62.48	78.20

compounds were infused in MS system by flushing with methanol (MeOH) in CE system. The sheath liquid (MeOH/water 1:1 v/v with 0.1% of formic acid) was delivered at 0.01 mL/min flow using a LC isocratic pump (1260 Infinity, Agilent Technologies, Waldbronn, Germany). MS system was operated under positive ionization mode applying an electrospray voltage of 3 kV. Nitrogen was used as drying gas at 250 °C, with a flow rate of 6 L/min; the pressure of the nebulizer gas was set at 15 psig. Selected ion monitoring (SIM) mode was used to identify the studied compounds. In order to perform sample infusion into the quadrupole MS, a fused-silica capillary outer coated with polyimide (Polymicro Technologies, Phoenix, USA) of 100 cm length and internal diameter of 50 μm was used. The new capillary was conditioned by flushing with 1.0 $molL^{-1}$ NaOH (10 min), followed by water (10 min), and MeOH (15 min). Samples were injected hydrodinamically at 50 mbar for 2.0 s and cassette temperature was maintained at 25 °C. Among sample injections, a short capillary preconditioning was performed by flushing with 1 $molL^{-1}$ NaOH (1 min), followed by water (1 min) and MeOH (4 min). Data processing was performed on Agilent ChemStation for CE-MS software.

An Agilent 7100 capillary electrophoresis instrument (Palo Alto, USA) equipped with a DAD set at 210 nm (peak width >0.10 min; 2.0 s response time; 2.5 Hz), and a data acquisition and treatment software (HP ChemStation, rev A.06.01) was used to carry out all capillary zone electrophoresis (CZE) experiments. The capillary temperature was maintained at 25 °C, the samples were hydrodynamically injected (25 mbar for 5.0 s) and the electrophoretic system was operated under constant and negative voltage of -25 kV. For all experiments, a fused silica capillary with external polyimide coating was used (Polymicro Technologies, Phoenix, USA) with a 35 cm total length (26.5 cm effective length), 75 μm of internal diameter and 375 μm outside diameter. When a new capillary was used, it was conditioned by flushing with 1.0 mol L^{-1} of NaOH solution (30 min), deionized water (15 min) and background electrolyte (BGE) (15 min). In between runs, the capillary was flushed with fresh BGE (2 min).

3. Results and discussion

Our studies raised by the catalyst dispersion into solution containing methylene blue. This procedure was performed by exposing the solution with the dye in ultrasound before going to the UV emission chamber. In this way, a test was carried out during four sonication times, 5, 10, 15 and 20 min. Times less than 15 min did not indicate linearity, possibly due to low catalyst dispersion, therefore, these data were not reliable. Above this time, the results were linear and therefore more reliable. The optimal time of exposure to ultrasound was 15 min.

The relationship between absorbance and irradiation time of MB degradation using the catalyst were carried out under UVA irradiation in the UV-Box. The strong absorption band of MB located at $\lambda = 664$ nm decreases gradually upon increasing irradiation time. The absorbance of MB achieves almost 65% after 60 min of irradiation when 1.5 mg mL^{-1} of catalyst is utilized. The following results indicate that the concentration of catalyst required to obtain the best degradation results is up to 1.5 mg mL^{-1} of catalyst. Values lower than that, specifically 0.5, 1.0 mg mL^{-1}

Table 3. Percentage comparison of degradation of MB between UVA and sunlight in the mineralization process.

Time (min.)	% Degradation	
	UV Box	Sunlight
1 h	62.48	78.20
2 h	65.80	90.36
3 h	70.24	98.80
7 h	90.88	-
9 h	95.52	-

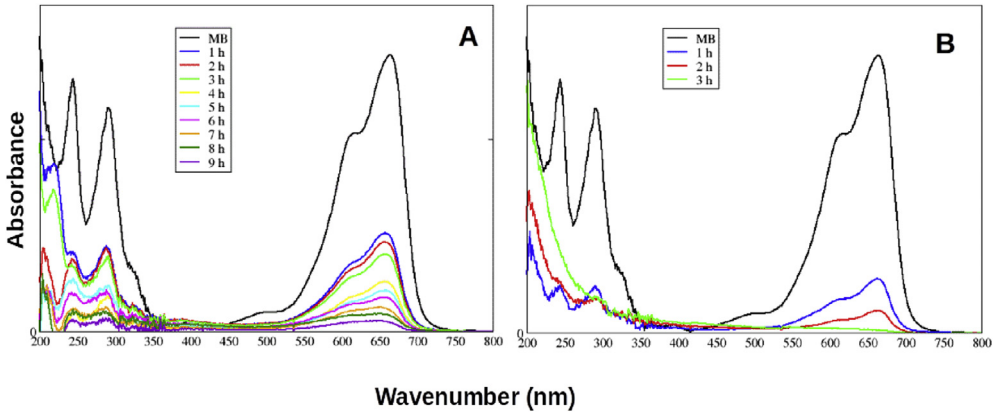

Figure 1. Photocatalytic activity of catalyst for degradation. A) UV Box B) Sunlight.

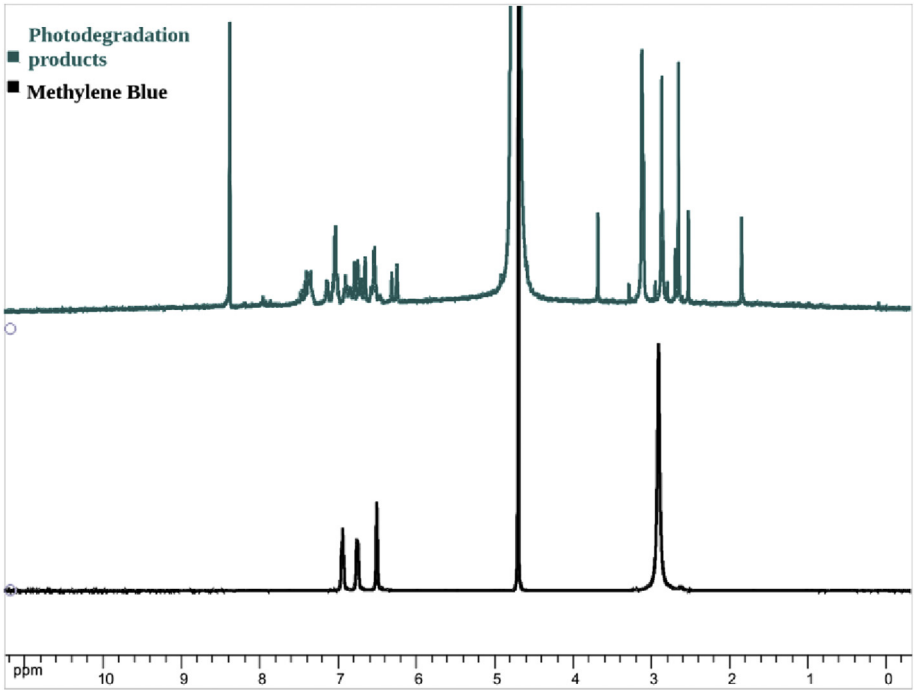

Figure 2. ^{1}H NMR (500 MHz, D_2O) spectrum of ^{1} photodegradation products and MB.

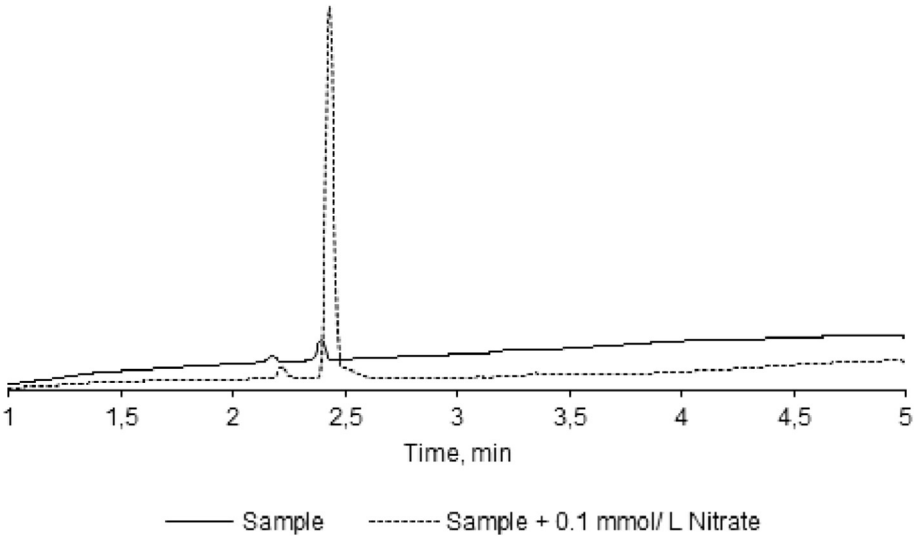

Figure 3. Electropherograms for NO_3^-: (–) indicates methylene blue sample; (---) indicates methylene blue sample added with standard solution of 0.1 mmol L^{-1} of NO_3^-. BGE: 40 mmol L^{-1} of TRIS and 20 mmol L^{-1} HCl (pH 8.20).

degradation does occur, but only around 40%, even considering times greater than 60 min.

When catalyst at 1.5 mg mL^{-1} is used, the absorption peak at $\lambda = 664$ nm diminishes sharply after 40 min of irradiation and reaches 62.48% in 60 min. This phenomenon occurs due to the increase of photon absorption, which generates more electron-hole pairs, and consequently, increases photodegradation activity.

Above this concentration, e.g., 2.0 mg mL^{-1} of catalyst, the activity was kept constant. This fact can be explained by absorption and scattering of light by Nb_2O_5 particles, which decreases light intensity in the reaction medium [25]. These observations can be explained in terms of availability of active sites on the catalyst surface and the penetration of UV light into the suspension [26]. The total active surface area increases with increasing catalyst dosage. At the same time, due to an increase in the turbidity of the suspension, there is a decrease in UV light penetration as a result of increased scattering effect and hence the photo-activated volume of suspension decreases [27]. It is also worth noting that at concentrations greater than 1.5 mg mL^{-1}, an early precipitation of the catalyst is observed, which probably reaches the limit of dispersion and consequently limit of catalytic surface reaches, leading to similar results in higher concentration.

In order to evaluate the photocatalytic ability of support, Nb_2O_5 and the supported Nb_2O_5, control experiments were carried out (Table 1). The results clearly indicate a great improvement on degradation process under the design supported Nb_2O_5 as catalyst. The degradation percentage values of the support and Nb_2O_5 bulk were around 30% after 1 h of exposure, while the catalyst reached values close to 63%. The supported Nb_2O_5 showed an enhanced photocatalytic activity when

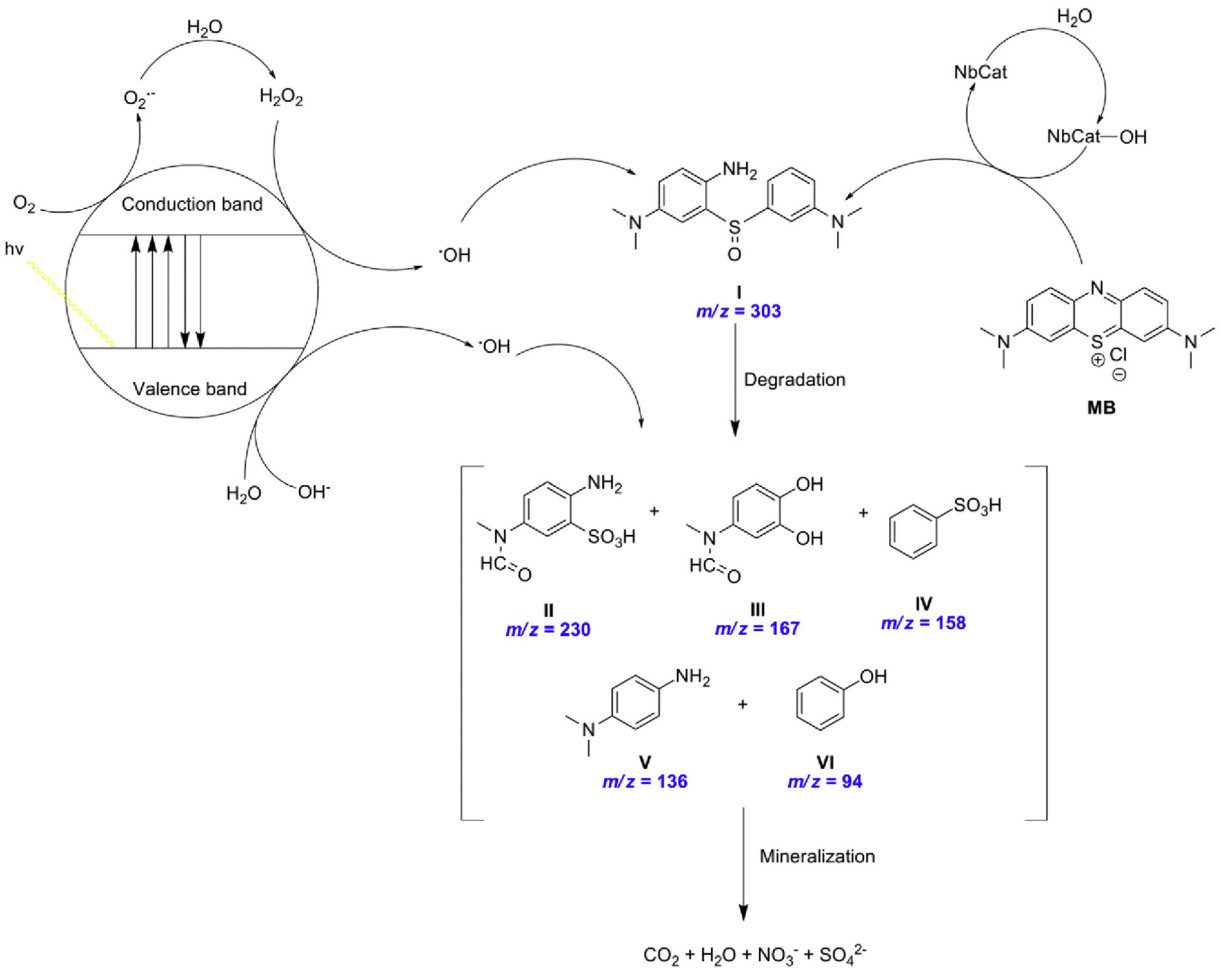

Scheme 1. Photocatalytic degradation pathway of MB.

compared with Nb_2O_5 bulk, probably to the large surface area which arises from the dispersion of catalytic phase in mixed oxides, improving the viability of catalytic sites of Nb_2O_5. In addition, high surface area may result in an enhanced absorption of MB. It is important to mention, control experiments revealed no degradation process neither by heating the MB solution at 80 °C for 10 h in a dark chamber or by exposing the MB solution at UV-box without the catalyst for 10 h. In addition, a solution of MB in the presence of mixed oxide precursor and Nb_2O_5 bulk revealed near the same percentage degradation considering the isolated species.

Viability studies of recovery of the catalyst and recycle test were performed (Table 1). The recycling studies revealed that the activity of catalyst maintained around 60% of dye degradation after three catalytic cycles, evidencing the Nb_2O_5 supported in mixed oxides can be reapplied in photodegradation reactions. This ability goes towards one of the key principles of green chemistry [28]. In addition, it is important to note that the supported catalyst has led to very interesting results with a decrease in the Nb_2O_5 content required for photodegradation. Another fact to be emphasized is that the light emission is in the range of UVA (315–400 nm), which is much less energetic and less harmful than the traditional UVC (100–280 nm), likely used in this kind of process. Besides, there is no need to add any additive in the photodegradation process, such as H_2O_2 or inorganic acids. This consists a great advantage of this methodology in comparison to others described in literature.

Having the UV-Box results in hand, the decomposition of MB in presence of sunlight was investigated (Table 2). To our delight, only 5 min was possible to observe almost 45% of dye degradation. Increasing the time to 60 min, 78.20% of degradation was detected. A good example of the great increase of dye degradation is the comparison between experiments collected in 30 min after sunlight exposure and 60 min in UV Box. They are basically in the same percentage of degradation, enhancing the activity after sunlight exposure.

In order to evaluate the possible resulting products in the photodegradation process of MB, a long exposure experiment was carried out. To this end, the same reaction condition was kept with a catalyst loading concentration of 1.5 mg mL^{-1} (Figure 1, Table 3).

As a result, after 120 min of exposure, a significant decrease in all signals was observed, even those at 200 nm, likely corresponding to aromatic compounds. This result indicates a degradation of aromatic compounds derived from MB. In this way, the presented methodology leads to almost complete mineralization of sample.

It is important to mention that recent reports in literature show supported semiconductor bimetallic composites leading to similar results; however, in those methods, quantitative amounts of both hydrogen peroxide (H_2O_2) or mineral acids are required in the reaction [29, 30].

After all these achievements, we then turned our attention into the study of plausible intermediates generated during the degradation process. To this end, an uncomplete experiment was carried out in the presence of deuterated water. Through the NMR analysis of photodegradation products spectrum (Figure 2) was possible to observe absorption signals between $\underline{\delta}$ 1.4–3.5 ppm referent to methyl groups present in its structures, while in the MB spectrum this region showed only one signal around $\underline{\delta}$ 3.0 ppm, indicating the presence of expected degradation of probe molecule. Signals corresponding to region from $\underline{\delta}$ 6.0–8.0 ppm were attributed to aromatic hydrogens present in the structure of intermediate products, corroborating with degradation process. Besides, it is

clear to observe an absorption signal at δ 8.3 ppm referent to hydrogen from intermediates which can be attributed to formamide moieties.

In order to identify nitrate ion (NO_3^-) in the methylene blue sample, a standard addition procedure by using capillary zone electrophoresis (CZE) equipment was carried out [31]. Operational conditions: cartridge temperature: 25 °C, injection pressure: 25 mbar for 5 s, wavelength: 210 nm and applied voltage: - 25 kV. Fused silica capillary with external polyimide coating containing 35 cm of total length (26.5 cm effective length) x 75 μm of internal diameter x 375 μm of external diameter. Control experiments were performed where fully degraded samples were produced and direct submitted to the CZE analyses. Electropherograms show the increase of peak signal for NO_3^- anion in methylene blue sample when submitted to the spiking test (Figure 3). This test is useful to confirm the presence of NO_3^- in the methylene blue sample. It is important to mention, a water solution containing only the catalyst was analyzed under the same CZE conditions and show no signal for NO_3^-.

Following the NMR and CZE analyses, LC/MS merges as a powerful tool to intercept plausible intermediates (Scheme 1). According to the literature, the initial step of MB degradation can be described as the catalyst promoted-oxidation of the C–S^+=C functional group to C–S-(=O)–C [11, 32], giving the plausible ring-opening intermediate which has been identified at m/z = 303. Then, subsequent attacks by ·OH radical produce the second and definitive dissociation of the two benzenic rings. These rings continue to suffer ·OH attacks giving rise the benzenic rings intermediates. These metabolites were identified at m/z = 230, 167, 158, 136 e 94. However, the species detected at m/z = 96 and 62, respectively SO_4^{2-} and NO_3^- suggests that ·OH radical attacks these organic species and can be further decomposed into these small molecules. These results corroborate with both UV-Vis and CZE analyses and evidence that a mineralization process may be happening. The complete degradation, or mineralization, leads to the conversion of organic carbon into harmless gaseous CO_2 and that of nitrogen and sulfur heteroatoms into inorganic ions, such as nitrate ions. This data may be indicative of the occurrence of this phenomenon, leading us to believe that it is a very promissory AOP.

4. Conclusions

In summary, additive and acid free Nb_2O_5 supported on mixed oxides photocatalyzed degradation of highly resistant organic dye is described. Furthermore, this heterogeneous photocatalysis process brings an important characteristic; the catalyst can be easily recovered and recycle for at least three times without any significant loss in terms of activity. Most impressive, the method is well conducted in the presence of highly abundant sunlight as energy source and the organic dye is degraded after only 3 h of exposure. Besides, this process is able to convert organic pollutants, in this case, methylene blue, into not harmful products without the need of heating, oxidants and chemical reactants. Plausible degradation intermediates were intercept and identified by NMR, LC/MS and CZE techniques.

Declarations

Author contribution statement

Gustavo Senra Gonçalves de Carvalho, Marcone Augusto Leal de Oliveira, Giovanni Wilson Amarante: Conceived and designed the experiments; Performed the experiments; Analyzed and interpreted the data; Contributed reagents, materials, analysis tools or data; Wrote the paper.

Marcelo Magno de Siqueira, Maria Patrícia do Nascimento: Conceived and designed the experiments; Performed the experiments; Analyzed and interpreted the data; Contributed reagents, materials, analysis tools or data.

Funding statement

This research did not receive any specific grant from funding agencies in the public, commercial, or not-for-profit sectors.

Competing interest statement

The authors declare no conflict of interest.

Additional information

No additional information is available for this paper.

Acknowledgements

We are grateful for research fellowships from CAPES (Finance Code 001), CNPq and FAPEMIG. The authors also acknowledge CBMM for ammoniacal niobium oxalate donation.

References

[1] A.R. Khataee, M.B. Kasiri, Photocatalytic degradation of organic dyes in the presence of nanostructured titanium dioxide: influence of the chemical structure of dyes, J. Mol. Catal. A Chem. 328 (2010) 8–26.
[2] S. Mancipe, F. Tzompantzi, H. Rojas, R. Gómez, Photocatalytic degradation of phenol using MgAlSn hydrotalcite-like compounds, Appl. Clay Sci. 129 (2016) 71–78.
[3] L.D.L. Miranda, C.R. Bellato, J.L. Milagres, L.G. Moura, A.H. Mounteer, M.F. Almeida, Hydrotalcite-TiO_2 magnetic iron oxide intercalated with the anionic surfactant dodecylsulfate in the photocatalytic degradation of methylene blue dye, J. Environ. Manag. 156 (2015) 225–235.
[4] M.A. Rauf, S. Salman Ashraf, Fundamental principles and application of heterogeneous photocatalytic degradation of dyes in solution, Chem. Eng. J. 151 (2009) 10–18.
[5] Z. Yang, F. Wang, C. Zhang, G. Zeng, X. Tan, Z. Yu, Y. Zhong, H. Wang, F. Cui, Utilization of LDH-based materials as potential adsorbents and photocatalysts for the decontamination of dyes wastewater: a review, RSC Adv. 6 (2016) 79415–79436.
[6] A. Kunz, P.P. Zamora, S.G. Moraes, N. Durán, Novas tendências no tratamento de efluentes têxteis, Quím. Nova 25 (2002) 78–82.
[7] M. Karkmaz, E. Puzenat, C. Guillard, J.M. Herrmann, Photocatalytic degradation of alimentary azo dye amaranth. Mineralization of the azo groupnitrogen, Appl. Catal. B Environ. 51 (2004) 183–194.
[8] R.P. Souza, T.K.F.S. Freitas, F.S. Domingues, O. Pezoti, E. Ambrosio, A.M. Ferrari-Lima, J.C. Garcia, Photocatalytic activity of TiO_2, ZnO and Nb_2O_5 applied to degradation of textile wastewater, J. Photochem. Photobiol. A 329 (2016) 9–17.
[9] a X. Lang, X. Chen, J. Zhao, Heterogeneous visible light photocatalysis for selective organic transformations, Chem. Soc. Rev. 43 (2014) 473–486;
b H.R. Mardani, M. Forouzani, M. Ziari, P. Biparva, Visible light photo-degradation of methylene blue over Fe or Cu promoted ZnO nanoparticles, Spectrochim. Acta Part A Mol. Biomol. Spectrosc. 141 (2015) 27–33;
c H.R. Mardani, (Cu/Ni)-Al layered double hydroxides@Fe3O4 as efficient magnetic nanocomposite photocatalyst for visible-light degradation of methylene blue, Res. Chem. Intermed. 43 (2017) 5795–5810.
[10] N.T. Prado, L.C.A. Oliveira, Nanostructured niobium oxide synthetized by a new route using hydrothermal treatment: high efficiency in oxidation reactions, Appl. Catal. B 205 (2017) 481–488.
[11] S. Xia, L. Zhang, G. Pan, P. Qiana, Z. Ni, Photocatalytic degradation of methylene blue with a nanocomposite system: synthesis, photocatalysis and degradation pathways, Phys. Chem. Chem. Phys. 17 (2015) 5345–5351.
[12] I. Nowak, M. Ziolek, Niobium compounds: preparation, characterization, and application in heterogeneous catalysis, Chem. Rev. 99 (1999) 3603–3624.
[13] S. Kuriakose, N. Bhardwaj, J. Singh, B. Satpati, S. Mohapatra, Structural, optical and photocatalytic properties of flower-like ZnO nanostructures prepared by a facile wet chemical method, Beilstein J. Nanotechnol. 4 (2013) 763–770.
[14] J. Chen, J. Cen, X. Xu, X. Li, The application of heterogeneous visible light photocatalyst in organic synthesis, Catal. Sci. Technol. 6 (2015) 349–362.
[15] G. Palmisano, V. Augugliaro, M. Pagliaro, L. Palmisano, Photocatalysis: a promising route for 21st century organic chemistry, Chem. Commun. (2007) 3425–3437.
[16] Y. Zhao, S. Zhang, B. Li, H. Yan, S. He, L. Tian, W. Shi, J. Ma, M. Wei, D.G. Evans, X. Duan, A family of visible-light responsive photocatalysts obtained by dispersing CrO_6 octahedra into a hydrotalcite matrix, Chem. Eur J. 17 (2011) 13175–13181.
[17] M.A. Abdel-Rehim, A.C.B. Santos, V.L.L. Camorin, A.C. Faro, Acid–base reactions on alumina-supported niobia, Appl. Catal. A 305 (2006) 211–218.
[18] L.C.A. Oliveira, T.C. Ramalho, E.F. Souza, M. Gonçalves, D.Q.L. Oliveira, M.C. Pereira, J.D. Fabris, Catalytic properties of goethite prepared in the presence

of Nb on oxidation reactions in water: computational and experimental studies, Appl. Catal. B Environ. 83 (2008) 169–176.
[19] L.H. Chagas, G.S.G. De Carvalho, W.R. Do Carmo, R.A.S. San Gil, S.S.X. Chiaro, A.A. Leitão, R. Diniz, L.A. De Sena, C.A. Achete, MLCoAl and NiCoAl LDHs synthesized by the hydrothermal urea hydrolysis method: structural characterization and thermal decomposition, Mater. Res. Bull. 64 (2015) 207–215.
[20] T.E. Johnson, W. Martens, R.L. Frost, Z. Ding, T. Kloprogge, Structured water in hydrotalcites of formula $MgxZn_6-xAl_2(OH)_{16}(CO_3)\cdot 4H_2O$: a Raman microscopic study, J. Raman Spectrosc. 33 (2002) 604–609.
[21] G.S.G. De Carvalho, L.H. Chagas, C.G. Fonseca, P.P. De Castro, A.C. Sant'Ana, A.A. Leitão, G.W. Amarante, Nb_2O_5 supported on mixed oxides catalyzed oxidative and photochemical conversion of anilines to azoxybenzenes, New J. Chem. 43 (2019) 5863–5871.
[22] F. Cavani, F. Trifirò, A. Vaccari, A hydrotalcite-type anionic clays: preparation and applications, Catal. Today 11 (1991) 173–301.
[23] S. Miyata, Physico-chemical properties of synthetic hydrotalcites in relation to composition, Clay Clay Miner. 28 (1980) 50–56.
[24] F.A.S. Vaz, M.A.L. Oliveira, M.P.G. Queiroz, S.J.L. Ribeiro, Construção de câmara de luz ultravioleta para fotopolimerização de fases estacionárias monolíticas, Quím. Nova 31 (2008) 2156–2158.
[25] Y. Zang, R. Farnood, Photocatalytic decomposition of methyl tert-butyl ether in aqueous slurry of titanium dioxide, Appl. Catal. B 57 (2005) 275.
[26] M.S.T. Goncalves, A.M.F. Oliveira-Campos, E.M.M.S. Pinto, P.M.S. Plasencia, M.J.R.P. Queiroz, Photochemical treatment of solutions of azo dyes containing TiO_2, Chemosphere 39 (1999) 781–786.
[27] N. Daneshvar, D. Salari, A.R. Khataee, Photocatalytic degradation of azo dye acid red 14 in water on ZnO as an alternative catalyst to TiO_2, J. Photochem. Photobiol. A 162 (2004) 317–322.
[28] A.G.S. Prado, Química verde, os desafios da química do novo milênio, Quím. Nova 26 (2003) 738–744.
[29] X. Yang, W. Chen, J. Huang, Y. Zhou, Y. Zhu, C. Li, Rapid degradation of methylene blue in a novel heterogeneous Fe_3O_4@rGO@TiO_2-catalyzed photo-Fenton system, Sci. Rep. 5 (2015) 10632.
[30] L. Wolski, M. Ziolek, Insight into pathways of methylene blue degradation with H2O2 over mono and bimetallic Nb, Zn oxides, App. Catal. B 224 (2018) 634–664.
[31] L.M. Duarte, T.L. Amorim, L.H. Adriano, M.A.L. Oliveira, Baseline separation of α and β-acids homologues and isomers in hop (*Humulus lupulus L.*) by CD-MEKC-UV, Electrophoresis 40 (2019) 1779–1786.
[32] A. Houas, H. Lachheb, M. Ksibi, E. Elaloui, C. Guillard, J.-M. Herrmann, Photocatalytic degradation pathway of methylene blue in water, App. Catal. B 31 (2001) 145–157.